NANO LETTERS

LETTER

pubs.acs.org/NanoLett

Achieving High Efficiency Silicon-Carbon Nanotube Heterojunction Solar Cells by Acid Doping

Yi Jia,[†] Anyuan Cao,[*,‡] Xi Bai,[†] Zhen Li,[†] Luhui Zhang,[‡] Ning Guo,[†] Jinquan Wei,[†] Kunlin Wang,[†] Hongwei Zhu,[†] Dehai Wu,[*,†] and P. M. Ajayan[§]

[†]Key Laboratory for Advanced Materials Processing Technology and Department of Mechanical Engineering, Tsinghua University, Beijing 100084, People's Republic of China

[‡]Department of Advanced Materials and Nanotechnology, College of Engineering, Peking University, Beijing 100871, People's Republic of China

[§]Department of Mechanical Engineering and Materials Science, Rice University, Houston, Texas 77005, United States

Supporting Information

ABSTRACT: Various approaches to improve the efficiency of solar cells have followed the integration of nanomaterials into Si-based photovoltaic devices. Here, we achieve 13.8% efficiency solar cells by combining carbon nanotubes and Si and doping with dilute HNO_3. Acid infiltration of nanotube networks significantly boost the cell efficiency by reducing the internal resistance that improves fill factor and by forming photoelectrochemical units that enhance charge separation and transport. Compared to conventional Si cells, the fabrication process is greatly simplified, simply involving the transfer of a porous semiconductor-rich nanotube film onto an n-type crystalline Si wafer followed by acid infiltration.

KEYWORDS: Carbon nanotube, solar cell, acid doping, photoelectrochemical cells

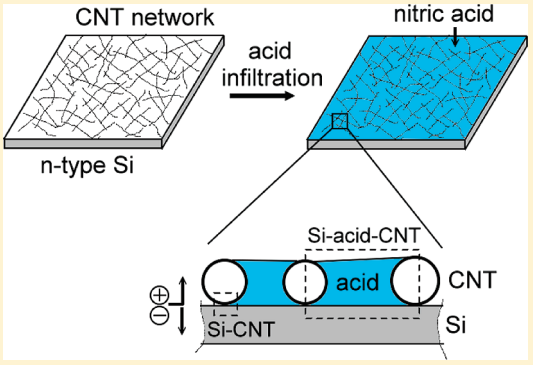

There has been a tremendous interest in developing next-generation photovoltaics based on advanced materials such as quantum dots, semiconducting nanostructrues, and conjugated polymers.[1−7] Crystalline silicon remains the basic material for high-efficiency stable photovoltaics, and recently it has been demonstrated that Si nanowire junctions or Si wire arrays from catalytic growth or electroless chemical etching can improve light absorption and radial charge collection in photovoltaic devices and also serve as electrodes for photoelectrochemical cells with efficiencies in the range of 1 to 8%.[8−12] On the other hand, integration of different nanostructures or polymers into Si-based photovoltaics has been explored widely and many heterojunction structures have been reported, such as GaN nanorods epitaxially grown on n-type Si,[13] InAs nanorods grown on p-type Si,[14] multiwalled nanotube array grown in anodized alumina template on Si substrate,[15] and polymeric materials and molecules coated on Si,[16,17] although the power conversion efficiencies of these devices are still low (<3%). Despite these advances, fabrication of photovoltaic devices surpassing the economic efficiency barrier (10%) by simple methods and at acceptable costs remains a grand challenge.[1]

Carbon nanotubes (CNTs) have high carrier mobility and can be interconnected into two-dimensional networks with tunable electrical and optical properties. Recently, we have demonstrated that coating a CNT film on n-type Si results in Si-CNT heterojunction solar cells with efficiencies up to 7%.[18] Compared with p-n junction Si modules and devices incorporating other nanomaterials on Si, our Si-CNT structure holds several advantages and potentially could lead to low-cost and high-efficiency solar cells. First, the CNT film acts as the p-type layer to form heterojunction with n-type Si and enable charge separation, removing the high-temperature diffusion and element doping steps in traditional Si cell fabrication.[19] Second, the two-dimensional conductive CNT network also serves as the transparent electrode for charge collection and transport, therefore metal wiring from the device surface that usually blocks a portion of incident light is no longer necessary. Other structures consisting of semiconducting nanowire arrays grown on Si still need a common top electrode because individual nanowires are well separated.[13,14] Third, the efficiency of our Si-CNT cells can be further improved by tailoring the composition (metallic tubes versus semiconducting tubes) and thickness of the CNT film to optimize the electronic and optical properties, as well as by chemical functionalization of CNTs.[20,21] Last, the Si-CNT model can be extended to other similar materials or structures, for example, we have recently reported Si-graphene solar cells,[22] CdSe nanobelt-Si cells,[23] and Si nanowire-CNT photoelectrochemical cells.[24] These studies also show the possibility to combine CNTs with Si nanowires or semiconducting nanobelts to form all-nanostructure solar cells.[23,24]

Received: November 12, 2010
Revised: March 22, 2011
Published: March 31, 2011

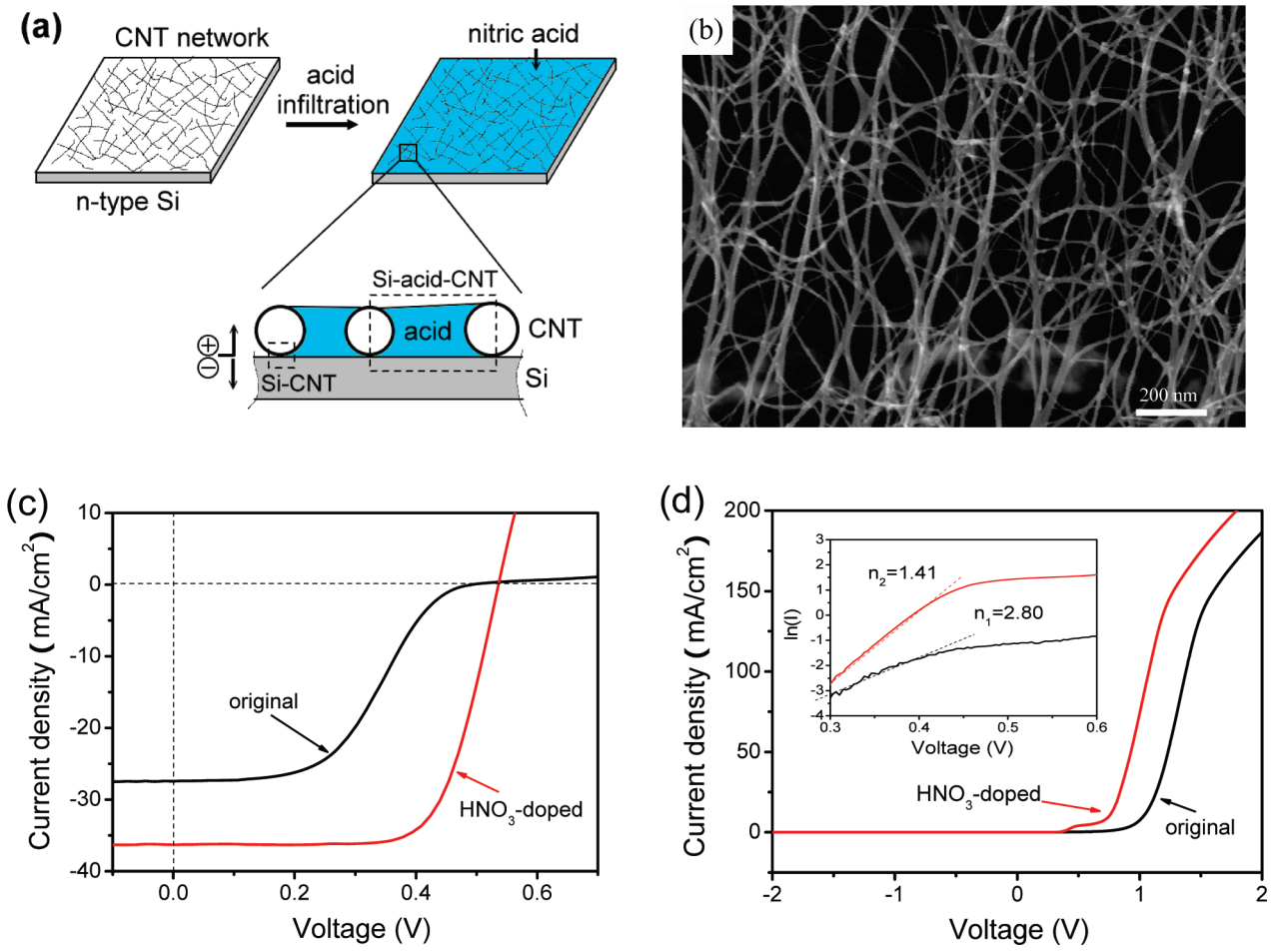

Figure 1. HNO_3 doping and cell efficiency improvement in Si-CNT solar cells. (a) Illustration of the solar cell structure based on a CNT network coated on an n-type Si wafer and infiltration of nitric acid into the network to form Si-acid-CNT photoelectrochemical units in addition to Si-CNT heterojunctions at the interface. (b) SEM image of the CNT film showing a porous network morphology. (c) $J-V$ characteristics of the solar cell before (black curve) and after (red) infiltration of dilute HNO_3. (d) Dark $J-V$ curves of the same cell before (black) and after (red) acid doping. Inset, plot of $\ln(I)$ versus voltage showing diode ideality factors before (n_1) and after (n_2) doping.

Here, we report the achievement of high performance Si-CNT hybrid solar cells by acid doping of the porous CNT network to form numerous heterojunctions and photoelectrochemical units in parallel, and shows a very high power conversion efficiency of up to 13.8% under AM 1.5G, one solar illumination (100 mW/cm^2). We found that doping CNT films by infiltration of a dilute common acid (HNO_3) can significantly boost the device efficiency by reducing internal resistance and assisting charge carrier separation and transport. With nitric acid doping, we have been able to reproducibly make Si-CNT cells with efficiencies in the range of 11−13%.

Our Si-CNT hybrid solar cell consists of an acid-infiltrated CNT film deposited on an n-type Si wafer (Figure 1a, see experimental methods in Supporting Information for details). The CNT film contains mostly single-walled nanotubes and small bundles with an optical transmittance of >85%, sheet resistance of <200 Ω per square, and a film porosity of about 70% (Figure 1b).[25] A pristine Si-CNT cell shows a short-circuit current density (J_{sc}) of 27.4 mA/cm^2, a fill factor (FF) of 47%, and an efficiency (η) of 6.2% in the light (AM 1.5G, 100 mW/cm^2). With acid (0.5 mol/L HNO_3) infiltration, the efficiency of this cell in wet state increases to 13.8%, owing to simultaneous enhancement in J_{sc} (from 27.4 to 36.3 mA/cm^2) and FF (from 47 to 72%) (Figure 1c). Dark current density−voltage ($J-V$) characteristics reveal that the diode ideality factor (n) has been improved from 2.8 (without acid) to 1.4 (with acid) (Figure 1d). In addition, the series resistance (R_s) has dropped from 36 Ω (or 3.24 Ω·cm^2) in the pristine cell to 25 Ω (or 2.25 Ω·cm^2) in the doped cell, resulting in a very large FF (72%). The pronounced effect of acid doping is general and reproducible for our Si-CNT solar cells; in more than 10 cells tested here (with initial efficiencies of 6−7%), their efficiencies have been enhanced to 11−13% after acid infiltration.

Our solar cells can produce very large J_{sc} values up to 36.3 mA/cm^2. Light reflection measurements on the Si-CNT cells shows a high absorption of 70−90% through the visible and near-infrared range (<1100 nm), due to the coating of a CNT film on Si surface (Supporting Information Figure S1). Theoretical work has estimated that in a textured Si p-n junction cell with an efficiency of 29.8% the maximum J_{sc} is 42.2 mA/cm^2 under a light absorption in the range of 80−95% (based on 100 μm Si slab).[26] The J_{sc} in our Si-CNT cells is still lower than this limitation and might be further increased by improving the light absorption.

There are several factors that contribute to the high efficiencies of Si-CNT hybrid solar cells. First, the CNT film synthesized

dx.doi.org/10.1021/nl2002632 |*Nano Lett.* 2011, 11, 1901–1905

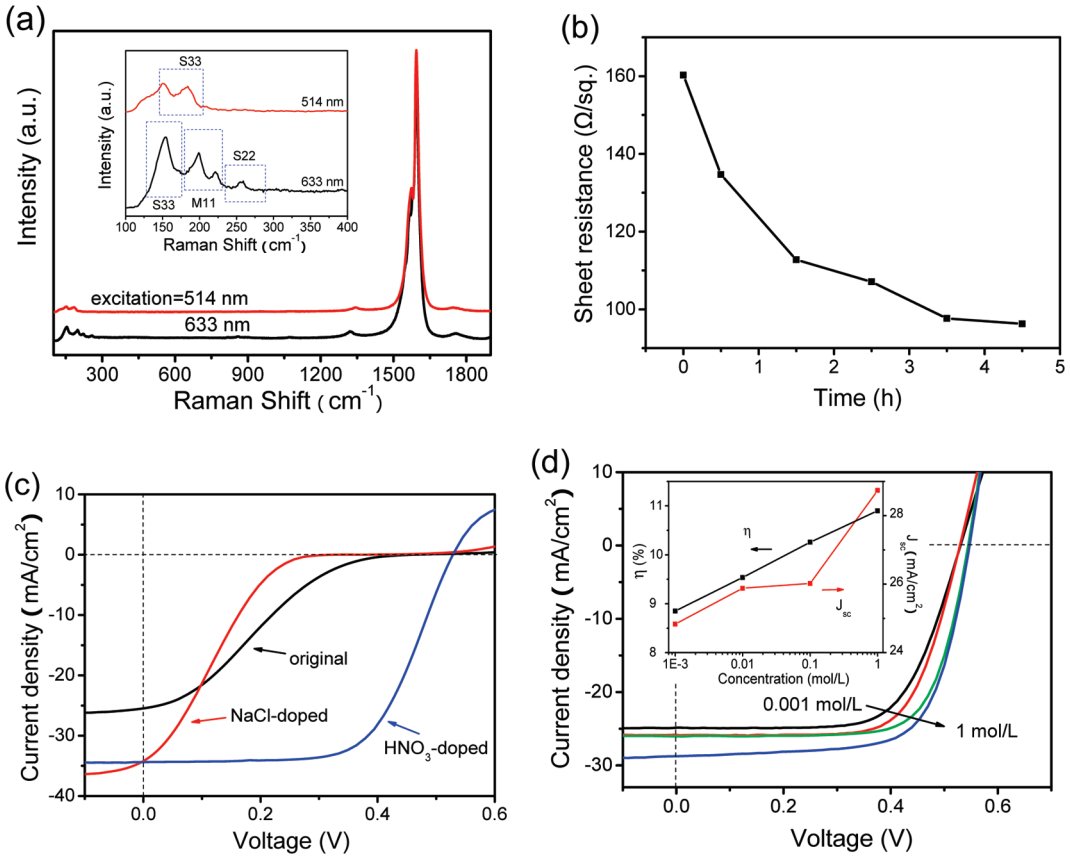

Figure 2. Mechanism for high efficiency Si-CNT solar cells. (a) Raman spectra of the CNT film recorded at excitation wavelengths of 514 and 633 nm, respectively. Inset, radial breathing mode peaks revealed in the spectra in which peaks of semiconducting nanotubes are marked in rectangles as "S33" or "S22" and those of metallic nanotubes are marked as "M11". (b) Sheet resistance of the CNT film measured after different periods of soaking in concentrated HNO_3. (c) $J-V$ curves of a Si-CNT cell in dry state (black curve), after infiltration of NaCl solution (red), and dilute HNO_3 (blue), respectively. (d) $J-V$ curves of a Si-CNT cell after infiltration of HNO_3 with different concentrations (from left to right, 0.001, 0.01, 0.1, and 1 mol/L). Inset shows the change of cell efficiency (η) and J_{sc} with increasing acid concentration.

in our chemical vapor deposition (CVD) process contains predominantly semiconducting nanotubes that can form heterojunctions with n-type Si for effective charge separation.[17] Raman spectra at excitations of different wavelengths show absence (514 nm) or relatively low intensity (633 nm) of peaks corresponding to metallic nanotubes (Figure 2a). Second, HNO_3 doping of the CNT network can reduce series resistance that is critical for obtaining large fill factors in solar cells.[27] In our planar device structure where a two-dimensional CNT film lays down on a Si wafer without top electrodes, the sheet resistance of the CNT layer accounts for the major internal series resistance because charge carriers are transported through the network to the outside and then collected. Immersing of CNT films in concentrated HNO_3 (15 mol/L) for 4 h has resulted in the decrease of sheet resistance by nearly 40%, from initially 160 to less than 100 Ω per square (Figure 2b). It has been observed by other groups that HNO_3 treatment caused decrease of CNT sheet resistance due to p-type doping and removal of residual molecules.[28,29] In addition, doping CNTs by other chemicals (thionyl chloride) to increase the carrier concentration and improve cell efficiency by 50% has been reported.[21]

Third, at the microscale acid infiltration resulted in the formation of Si-acid-CNT units in the pores of the CNT networks (illustrated in Figure 1a). The exposed Si surface in the empty areas of the CNT film now is covered by acid, and semiconductor−electrolyte interface forms. In a dry coating, many overlapped and suspended CNTs may not contact the Si substrate. The Si-acid-CNT units are formed in the areas involving Si photoanodes and CNT cathodes in the vicinity (including tube side-walls and suspended tubes/bundles) with the acid as aqueous electrolyte. If nitric acid can assist the extraction and transport of holes from Si to the CNT film, these Si-acid-CNT units actually work in a manner similar to (microscale) photoelectrochemcial (regenerative) cells.[30] A possible redox reaction here is hydrogen getting oxidized by scavenging holes from Si anode and protons getting reduced at the CNT surface by receiving electrons. Here the role of HNO_3 as the electrolyte can be further proved by making a Si-HNO_3-CNT structure where the CNT film was separated from Si by 300 nm with HNO_3 in between and demonstrating that this will work as a photoelectrochemical cell (Supporting Information Figure S2). Since all photoelectrochemical units and Si-CNT heterojunctions are connected in parallel on the same side of Si, there is no short circuit in the device. Given the high porosity of CNT films (~70%), one could expect substantial enhancement in cell efficiency by acid infiltration which simultaneously promotes charge separation at the interface and provide additional charge transport paths through the CNT network.

Infiltration by other liquids such as a salt solution did not yield the same effect as acid doping. We started from a dry Si-CNT

dx.doi.org/10.1021/nl2002632 |*Nano Lett.* 2011, 11, 1901–1905

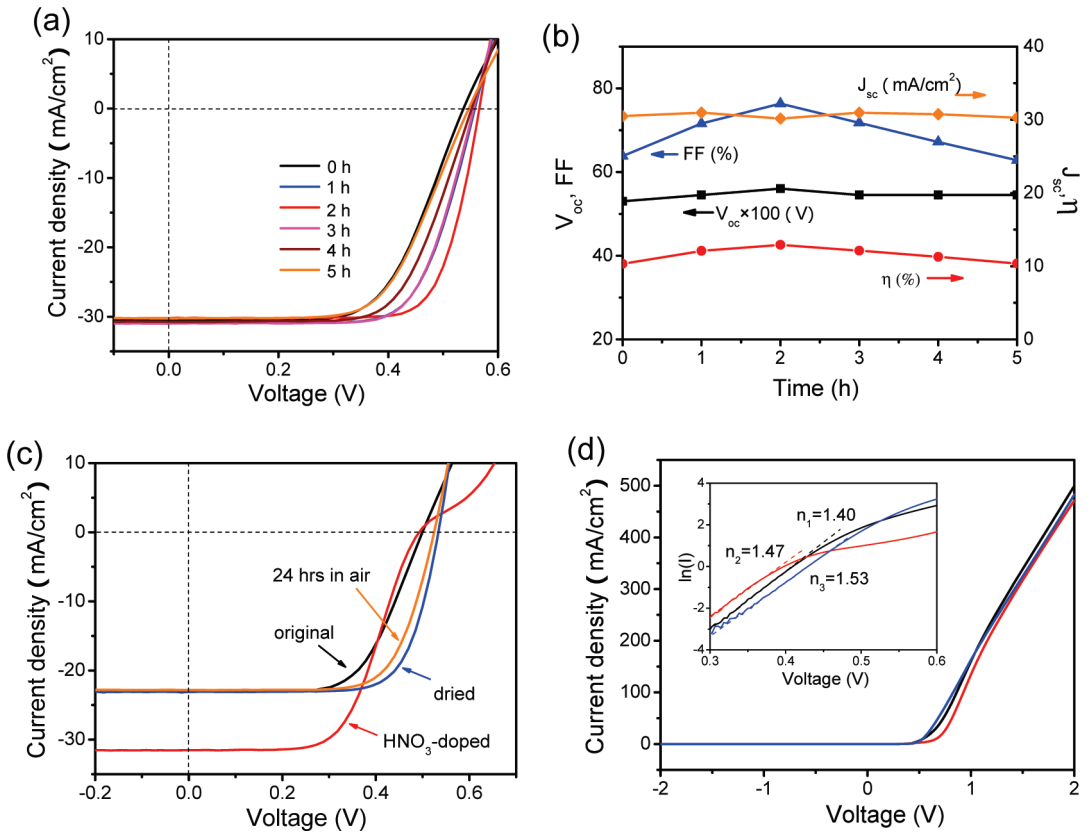

Figure 3. Stability and reversibility of HNO_3-doped Si-CNT cells. (a) $J-V$ curves recorded on a Si-CNT cell infiltrated by HNO_3 for 5 hours. (b) Calculated cell parameters during this period. (c) $J-V$ curves of a Si-CNT cell in pristine form (black), when doped with HNO_3 (red), in dry state after acid has vaporized (blue), and after 24 hours of exposure in air (orange). (d) Dark $J-V$ curves of the pristine cell (black), HNO_3-doped cell (red), and the dry cell (blue). Inset, diode ideality factors of the pristine (n_1), doped (n_2), and dried (n_3) cell.

solar cell with an efficiency of 2.6%, and infiltrated NaCl solution (0.1 mol/L) or HNO_3 (0.1 mol/L) with the same concentration, respectively. Although NaCl infiltration increases the current density from 25.4 to 34.2 mA/cm^2, the fill factor remains at a low level (19%) (Figure 2c). In contrast, HNO_3 not only increases the current density to 34.4 mA/cm^2, but also improves the fill factor to 65%, resulting in a cell efficiency of 11.5%. Even this cell has a relatively poor initial efficiency (2.6%), the acid infiltration readily enhanced the device to an efficiency of >10%. The S-shape in the higher voltage level (0.3−0.6 V) might originate from the Si-CNT interface because the CNT film was directly transferred to Si without further enhancement of contact. We have also observed similar doping effect from other nonvolatile acids, for example, infiltration of H_2SO_4 (0.1 mol/L) using the same procedure improved the Si-CNT cell efficiency from 6.2 to 10.4% (Supporting Information Figure S3). H_2SO_4 treatment could graft chemical functionalities on CNTs and enhance the network conductivity.[31] Furthermore, the effect of acid concentration has been investigated in the range of 0.001 to 1 mol/L. Starting from a single Si-CNT cell, infiltration of very diluted nitric acid (0.001 mol/L) resulted in a cell efficiency of 8.8%, and infiltration of more concentrated acid (1 mol/L) resulted in an efficiency of 10.9% (Figure 2d). The current density and cell efficiency has been improved consistently with increasing acid concentration within the studied range.

We have tested the stability of Si-CNT cells during the acid infiltration process for 5 h by recording a series of $J-V$ curves at one-hour interval. This cell has an initial FF of 63.8% and efficiency of 10.3%, and during the first 2 h, the $J-V$ curves shift toward right side with increasing FF up to 76.3% and efficiency up to 12.9% (Figure 3a). After that, we monitored a slight degradation of fill factor and a decrease of cell efficiency from 12.9 to 10.4% (close to initial value). The fill factor is changing here while the V_{oc} and J_{sc} are rather stable (Figure 3b). In the first 2 h, increase of fill factor is mainly attributed to the gradual infiltration process of HNO_3 and doping of CNTs, which correspondingly reduce the series resistance. In the following time, the drop of cell efficiency is probably due to the photocorrosion effects of Si in contact with strong acid. Under continuous illumination, the photocurrent dropped from about 29 to 27 mA/cm^2 after 20 min (Supporting Information Figure S4). The photocorrosion effect is under study, and it might be possible to introduce a thin oxide layer on the surface of Si to circumvent this issue for long time stability.

Since the acid used here is volatile, we studied the reversibility of Si-CNT solar cells in doped (wet) and undoped (dry) conditions. The tested cell had an initial J_{sc} of 23.1 mA/cm^2 and efficiency of 7.2%, which increased to 31.5 mA/cm^2 and 9.2%, respectively, after 0.1 mol/L acid doping (Figure 3c). Upon exposure to air, the cell efficiency drops to 8.9% when the nitric acid completely vaporized. In this dry state, the cell maintains a rather stable performance with slight decrease of efficiency (to 8.4%) after 24 h storage in air (Figure 3c). The dried cell after doping recovered to the same current density (J_{sc}) as that of its pristine form with slightly improved fill factor. Dark $J-V$ characteristics monitored during the acid drying process shows

dx.doi.org/10.1021/nl2002632 |*Nano Lett.* 2011, 11, 1901–1905

that the diode ideality factor increased slightly from 1.4 (with acid) to 1.47 (when acid vaporized) and then to 1.53 (after 24 h exposure in air), which might be the reason for modest efficiency degradation observed in this cell (Figure 3d). Infiltrating acid again leads to change of cell efficiency in a similar way to the first cycle, indicating that the acid doping of Si-CNT cells is a reversible process and cell efficiencies in both infiltrated and dry states can be controlled. Longer time stability tests show that the performance degradation is within 10% when the HNO_3-doped cell was in dry state and exposed to air for 10 days, in which the cell efficiency has dropped from 10.1 to 9.2% during this period (Supporting Information Figure S5).

To summarize, we have demonstrated high efficiency Si-CNT solar cells that can be reproducibly fabricated by coating a CNT film on Si substrate and doping the porous film with acid. Built on a basic cell structure consisting of semiconducting Si-CNT heterojunctions, the acid doping reduces the internal series resistance and provides more charge transport paths in the porous material, resulting in significantly improved cell efficiencies in the range of 11−13%. The device performance might be further improved by tailoring the electrical property and the film porosity of CNTs. For practical applications, stability issues related to Si photocorrosion and acid storage should be addressed, which might be circumvented by introduction of an oxide layer or mild acid electrolytes and better device encapsulation. The Si-CNT solar cells reported here are made by much simplified process compared with traditional Si cells while meeting the same basic efficiency requirement for solar cell commercialization and practical use.

■ ASSOCIATED CONTENT

Supporting Information. Materials and experimental methods and additional tables and figures. This material is available free of charge via the Internet at http://pubs.acs.org.

■ AUTHOR INFORMATION

Corresponding Author

*E-mail: (A.C.) anyuan@pku.edu.cn; (D.W.) wdh-dme@tsinghua.edu.cn.

■ ACKNOWLEDGMENT

This work was supported by 863 Program (No. 2009AA05Z423), National Science Foundation of China (NSFC) (No. 50972067), Research Fund for Doctoral Program of Ministry of Education of China (No. 20090002120019). A.C. acknowledges financial support from NSFC under Grant 51072005.

■ REFERENCES

(1) Lewis, N. S. *Science* **2007**, *315*, 798–801.
(2) Pattantyus-Abraham, A. G.; Kramer, I. J.; Barkhouse, A. R.; Wang, X.; Konstantatos, G.; Debnath, R.; Levina, L.; Raabe, I.; Nazeeruddin, M. K.; Grätzel, M.; Sargent, E. H. *ACS Nano* **2010**, *4*, 3374–3380.
(3) Tisdale, W. A.; Williams, K. J.; Timp, B. A.; Norris, D. J.; Aydil, E. S.; Zhu, X.-Y. *Science* **2010**, *328*, 1543–1547.
(4) Gur, I.; Fromer, N. A; Geier, M. L.; Alivisatos, A. P. *Science* **2005**, *310*, 462–465.
(5) Fan, Z.; Razavi, H.; Do, J.-W.; Moriwaki, A.; Ergen, O.; Chueh, Y.-L.; Leu, P. W.; Ho, J. C.; Takahashi, T.; Reichertz, L. A.; Neale, S.; Yu, K.; Wu, M.; Ager, J. W.; Javey, A. *Nat. Mater.* **2009**, *8*, 648–653.
(6) Shaheen, S. E.; Ginley, D. S.; Jabbour, G. E. *MRS Bull.* **2005**, *30*, 10–19.
(7) Kim, J. Y.; Lee, K.; Coates, N. E.; Moses, D.; Nguyen, T.-Q.; Dante, M.; Heeger, A. J. *Science* **2007**, *317*, 222–225.
(8) Tian, B.; Zheng, X.; Kempa, T. J.; Fang, Y.; Yu, N.; Yu, G.; Huang, J.; Lieber, C. M. *Nature* **2007**, *449*, 885–890.
(9) Sivakov, V.; Andrä, G.; Gawlik, A.; Berger, A.; Plentz, J.; Falk, F.; Christiansen, S. H. *Nano Lett.* **2009**, *9*, 1549–1554.
(10) Boettcher, S. W.; Spurgeon, J. M.; Putnam, M. C.; Warren, E. L.; Turner-Evans, D. B.; Kelzenberg, M. D.; Maiolo, J. R.; Atwater, H. A.; Lewis, N. S. *Science* **2010**, *327*, 185–187.
(11) Kelzenberg, M. D.; Boettcher, S. W.; Petykiewicz, J. A.; Turner-Evans, D. B.; Putnam, M. C.; Warren, E. L.; Spurgeon, J. M.; Briggs, R. M.; Lewis, N. S.; Atwater, H. A. *Nat. Mater.* **2010**, *9*, 239–244.
(12) Peng, K.-Q.; Wang, X.; Wu, X.-L.; Lee, S. T. *Nano Lett.* **2009**, *9*, 3704–3709.
(13) Tang, Y. B.; Chen, Z. H.; Song, H. S.; Lee, C. S.; Cong, H. T.; Cheng, H. M.; Zhang, W. J.; Bello, I.; Lee, S. T. *Nano Lett.* **2008**, *8*, 4191–4195.
(14) Wei, W.; Bao, X.-Y.; Soci, C.; Ding, Y.; Wang, Z.-L.; Wang, D. *Nano Lett.* **2009**, *9*, 2926–2934.
(15) Tzolov, M. B.; Kuo, T.-F.; Straus, D. A.; Yin, A.; Xu, J. *J. Phys. Chem. C* **2007**, *111*, 5800–5804.
(16) Khatri, I.; Adhikari, S.; Aryal, H. R.; Soga, T.; Jimbo, T.; Umeno, M. *Appl. Phys. Lett.* **2009**, *94*, 093509.
(17) Har-Lavan, R.; Ron, I.; Thieblemont, F.; Cahen, D. *Appl. Phys. Lett.* **2009**, *94*, 043308.
(18) Jia, Y.; Wei, J.; Wang, K.; Cao, A.; Shu, Q.; Gui, X.; Zhu, Y.; Zhuang, D.; Zhang, G.; Ma, B.; Wang, L.; Liu, W.; Wang, Z.; Luo, J.; Wu, D. *Adv. Mater.* **2008**, *20*, 4594–4598.
(19) Wenham, S. R.; Green, M. A. *Prog. Photovoltaics* **1996**, *4*, 3–33.
(20) Behnam, A.; Johnson, J. L.; Choi, Y.; Ertosun, M. G.; Okyay, A. K.; Kapur, P.; Saraswat, K. C.; Ural, A. *Appl. Phys. Lett.* **2008**, *92*, 243116.
(21) Li, Z.; Kunets, V. P.; Saini, V.; Xu, Y.; Dervishi, E.; Salamo, G. J.; Biris, A. R.; Biris, A. S. *ACS Nano* **2009**, *3*, 1407–1414.
(22) Li, X.; Zhu, H.; Wang, K.; Cao, A.; Wei, J.; Li, C.; Jia, Y.; Li, Z.; Li, X.; Wu, D. *Adv. Mater.* **2010**, *22*, 2743–2748.
(23) Zhang, L.; Jia, Y.; Wang, S.; Li, Z.; Ji, C.; Wei, J.; Zhu, H.; Wang, K.; Wu, D.; Shi, E.; Fang, Y.; Cao, A. *Nano Lett.* **2010**, *10*, 3583–3589.
(24) Shu, Q.; Wei, J.; Wang, K.; Zhu, H.; Li, Z.; Jia, Y.; Gui, X.; Guo, N.; Li, X.; Ma, C.; Wu, D. *Nano Lett.* **2009**, *9*, 4338–4342.
(25) Li, Z.; Jia, Y.; Wei, J.; Wang, K.; Shu, Q.; Gui, X.; Zhu, H.; Cao, A.; Wu, D. *J. Mater. Chem.* **2010**, *20*, 7236–7240.
(26) Tiedje, T.; Yablonovitch, E.; Cody, G. D.; Brooks, B. G. *IEEE Trans. Electron Devices* **1984**, *ED-31*, 711–716.
(27) Würfel, P. Physics of Solar Cells: From Principles to New Concepts. *Limitations on energy conversion in solar cells*; Weinheim, 2005; Chapter 7, pp 137−154.
(28) Shin, D.-W.; Lee, J. H.; Kim, Y.-H.; Yu, S. M.; Park, S.-Y.; Yoo, J.-B. *Nanotechnology* **2009**, *20*, 475703.
(29) Kaskela, A.; Nasibulin, A. G.; Timmermans, M. Y.; Aitchison, B.; Papadimitratos, A.; Tian, Y.; Zhu, Z.; Jiang, H.; Brown, D. P.; Zakhidov, A.; Kauppinen, E. I. *Nano Lett.* **2010**, *10*, 4349–4355.
(30) Grätzel, M. *Nature* **2001**, *414*, 338–344.
(31) Tantang, H.; Ong, J. Y.; Loh, C. L.; Dong, X.; Chen, P.; Chen, Y.; Hu, X.; Tan, L. P.; Li, L.-J. *Carbon* **2009**, *47*, 1867–1870.